

Technical Report

TR-12-05

Turbulent transport in the atmospheric surface layer

Torbern Tagesson

Department of Physical Geography and Ecosystem Science,
Lund University

April 2012

Svensk Kärnbränslehantering AB

Swedish Nuclear Fuel
and Waste Management Co

Box 250, SE-101 24 Stockholm
Phone +46 8 459 84 00



ISSN 1404-0344

SKB TR-12-05

ID 1348842

Turbulent transport in the atmospheric surface layer

Torbern Tagesson

Department of Physical Geography and Ecosystem Science,
Lund University

April 2012

Keywords: Atmosphere, Eddy diffusivity model, Canopy, Wind profile, CO₂.

This report concerns a study which was conducted for SKB. The conclusions and viewpoints presented in the report are those of the author. SKB may draw modified conclusions, based on additional literature sources and/or expert opinions.

A pdf version of this document can be downloaded from www.skb.se.

Abstract

In the modelling of transport and accumulation of the radioactive isotope carbon-14 (C-14) in the case of a potential release from a future repository of radioactive waste, it is important to describe the transport of the isotope in the atmosphere. This report aims to describe the turbulent transport within the lower part of the atmosphere; the inertial surface layer and the roughness sublayer. Transport in the inertial surface layer is dependent on several factors, whereof some can be neglected under certain circumstances. Under steady state conditions, fully developed turbulent conditions, in flat and horizontal homogeneous areas, it is possible to apply an eddy diffusivity approach for estimating vertical transport of C. The eddy diffusivity model assumes that there is proportionality between the vertical gradient and the transport of C. The eddy diffusivity is depending on the atmospheric turbulence, which is affected by the interaction between mean wind and friction of the ground surface and of the sensible heat flux in the atmosphere. In this report, it is described how eddy diffusivity of the inertial surface layer can be estimated from 3-d wind measurements and measurements of sensible heat fluxes. It is also described how to estimate the eddy diffusivity in the inertial surface layer from profile measurements of temperature and wind speed.

Close to the canopy, wind and C profiles are influenced by effects of the surface roughness; this section of the atmosphere is called the roughness sublayer. Its height is up to ~3 times the height of the plant canopy. When the mean wind interacts with the canopy, turbulence is not only produced by shear stress and buoyancy, it is additionally created by wakes, which are formed behind the plants. Turbulence is higher than it would be over a flat surface, and the turbulent transport is hereby more efficient. Above the plant canopy, but still within the roughness sublayer, a function that compensates for the effect of increased turbulence is included in the eddy diffusivity model. The turbulent transport gets complicated when we enter the plant canopy. The profiles are then not only affected by the changes in turbulence, but also by the spatial distribution of sinks and sources for C within the plant canopy. The exchange of C within the plant community mainly goes through the stomata of leafs. The sink and source distribution of C is hereby influenced by vertical and horizontal distribution of leaf area density and incoming radiation. Because of this sink and source distribution and the change in turbulence, the eddy diffusivity model is no longer applicable. An alternative model is briefly described, the Lagrangian model. The Lagrangian model aims to predict the probability that a moving air parcel in the canopy space will encounter a source or a sink of C. The C concentration will decrease when it passes a sink or increase if it passes a source. The aim is to predict the C concentration profile within the plant canopy.

Sammanfattning

Det är viktigt att beskriva hur den radioaktiva isotopen kol 14 (C-14) kan komma att ackumuleras och transporteras vid ett eventuellt framtida utsläpp i området där man planerar att anlägga ett djupförvar av utbränt kärnbränsle. Syftet med denna rapport är att beskriva den turbulenta transporten i atmosfärens lägsta lager; det konstanta fluxlagret och skrovlighetslagret. Transporten i det konstanta fluxlagret beror på flertalet faktorer, varav man kan ignorera vissa under särskilda omständigheter. Vid stationärt tillstånd, fullt utvecklad turbulens, och i platta och horisontellt homogena områden kan man applicera en diffusivitetsmodell för att skatta den vertikala transporten av C-14. Diffusivitetsmodellen antar att där finns en proportionalitet mellan den vertikala gradienten av C-14 och transporten av densamma. Diffusiviteten i atmosfären beror på turbulensen, som i sin tur påverkas av vindens medelhastighet, markens friktion och det sensibla värmeflödet. I rapporten beskrivs hur diffusiviteten i det konstanta fluxlagret kan skattas utifrån 3-dimensionella vindmätningar och fältmätningar av det sensibla värmeflödet. Det beskrivs även hur diffusiviteten kan skattas utifrån profilmätningar av temperatur och vindhastighet.

Atmosfärsdraget närmast marken kallas för skrovlighetslagret. Skrovlighetslagret kan sträcka sig så högt som 3 gånger höjden av markens växtlighet. När luft rör sig inom skrovlighetslagret skapas turbulens inte bara av friktion och av luftens bärcraft, det skapas även av svallvågor som formas bakom växterna. Turbulensen är härmed högre än det vore över en plan yta och den turbulenta transporten är också mer effektiv. Medan man befinner sig ovanför växternas krontak, men innanför skrovlighetslagret, kan man kompensera för denna effekt genom att lägga till en funktion i diffusivitetsmodellen. Det blir dock mer komplicerat när man skall beräkna flux inom växtbeståndet. Koldioxidprofilen påverkas då inte bara av turbulensen, utan även av den spatiala distributionen av kolsänkor och kolkällor. Koldioxidutbytet sker främst genom bladens klyvöppningar och distributionen av kolsänkor och kolkällor påverkas härmed av den vertikala och horisontella distributionen av blad och den inkommande solstrålningen. Diffusivitetsmodellen är inte längre applicerbar när man befinner sig inom växtbeståndet på grund av denna distribution av kolsänkor och kolkällor. En alternativ modell beskrivs ytligt i rapporten, den så kallade Lagrangianska modellen. Syftet med den Lagrangianska modellen är att förutsäga sannolikheten att ett luftpaket kommer att passera en kolsänka eller kolkälla som påverkar luftpaketets kolkoncentration. Koldioxidkoncentrationen kommer att öka om den passerar en kolkälla och den kommer att minska om den passerar en kolsänka. Syftet är att förutspå koldioxidens koncentrationsgradient och dess transport inom växtbeståndet.

Contents

1	Introduction	7
2	The planetary boundary layer	9
3	The inertial surface layer	11
3.1	Assumptions made for the eddy diffusivity approach to be valid	11
3.2	The wind profile under neutral conditions	11
3.3	The effect of plants and surface friction on the wind profile	12
3.4	The effect of diurnal variation on the wind profile	13
3.5	Atmospheric stability parameter	14
3.6	Monin-Obukhov similarity theory	15
3.7	Wind profiles under stable and unstable conditions	16
3.8	The eddy diffusion coefficient for momentum during neutral conditions	17
3.9	The eddy diffusion coefficient for momentum during different stability conditions	18
3.10	The temperature profile during different stability conditions	19
3.11	The eddy diffusion coefficient for sensible heat during different stability conditions	20
3.12	Profile measurements for estimating eddy diffusivity	21
4	The Roughness sublayer	23
4.1	Characteristics of the roughness sublayer	23
4.2	Turbulent transport above the canopy but within the roughness sublayer	24
4.3	Turbulent transport within the plant canopy	24
4.4	Carbon dioxide profiles within the plant canopy	25
4.5	Alternative modelling approaches	26
	Acknowledgements	29
	References	31
	Appendix 1	33

1 Introduction

The efforts to understand the exchange processes between the ground surface and the atmosphere mainly have two reasons. The first is to model microclimate, that is, flux and concentration profiles of atmospheric properties (e.g. heat, water vapour, carbon dioxide (CO₂)). This is done by using input parameters of the canopy and the atmosphere. The second motive is the opposite; if we know the exchange processes, we can try to understand the biological and physical properties of the plants on the surface we are studying (Raupach 1989a, b).

The transport within and above the plant canopy is to a large extent dependent on the turbulence of the atmosphere. The turbulent exchange occurs over a wide range of scales from millimetres to kilometres in size. These differently sized turbulent elements can be thought of as air parcels. These air parcels are called eddies and they have similar thermodynamic properties. Eddies transport energy and gases by their random motion in the atmosphere. There are a set of equations that describe the turbulent motions within the atmosphere. These turbulent equations of motions have several unknown parameters and differential equations (Foken 2008). To be able to solve these equations, several simplifications have been done. Different approaches have been used and they are called closure techniques. The closure technique that will be used in this report is the first-order closure technique, and it is analogous to the molecular diffusion approach. It assumes that there is proportionality between the vertical flux of a state variable (e.g. heat, water vapour, CO₂) and the vertical gradient of that specific state variable. This proportionality is also called the eddy diffusion coefficient, K , and this approach is therefore called the K -theory. If we know the flux of a property of the atmosphere, and we know the eddy diffusion coefficient, we can estimate the concentration gradient. We can also estimate the flux of an atmospheric property, if we know the eddy diffusion coefficient and the concentration gradient.

The K -theory is based on a couple of assumptions, and these assumptions are not valid within the plant canopy (Kaimal and Finnigan 1994). When the turbulent elements interact with the canopy, turbulence is increased. Large sized eddies are formed in the interaction between the mean wind and the top of the canopy. These are responsible for a large fraction of the turbulent transport within the canopy. Additionally, there are sinks and sources within the plant canopy. For example, CO₂ is respired from the soil surface through heterotrophic and root respiration. This is a source of CO₂. CO₂ is also respired from the trees through autotrophic respiration and the pathway is through leaves. However, the photosynthetic uptake also goes through leaves, and during daytime it is larger than the autotrophic respiration. Leaves in the canopy are hereby sinks during daytime but sources during nighttimes. With knowledge of the vertical sources and sinks throughout the canopy, the vertical concentration gradient can be estimated. This is done using the Lagrangian method (Raupach 1989b). It is also the other way around, if we know the concentration profile, we can estimate the source and sink profile in the canopy (Raupach 1989a).

This report is in a series of reports dealing with the modelling of transport and accumulation of the radioactive isotope C-14 in the case of a potential release from a future repository of radioactive waste in the Forsmark area. The aim is to review the vertical turbulent transport within the atmospheric surface layer. The report is constructed into two different sections. In the first part, it is discussed how eddy diffusion coefficients are estimated above the plant canopy in the inertial surface layer. In the second part, the transport and the CO₂ concentration profiles within and just above the canopy, in the roughness sublayer, is discussed.

2 The planetary boundary layer

The atmosphere near the surface of the earth can be divided into different layers. The upper layers are the free atmosphere, where the surface of the earth has no direct influence on the transport processes. Closest to the ground, we have the planetary boundary layer, where the exchange processes are affected by the friction of the surface of the earth. The planetary boundary layer is further divided into; the Ekman layer and the atmospheric surface layer. The free atmosphere and the Ekman layer is not affected by the processes described in this report. How the height of the surface layer is calculated is described in Kaimal and Finnigan (1994). The atmospheric surface layer is further divided into the inertial surface layer (above the plant canopy) and the roughness sublayer (within and just above the plant canopy). The inertial surface layer is also called the constant flux layer, and within it, the vertical turbulent fluxes are assumed to be constant with height. The height of the inertial surface layer is dependent on stability (see Section 3.5), and it stretches from a few meters under stable conditions up to 100 meters under unstable conditions. Close to the plant canopy, fluxes are affected by the roughness of the surface and the inertial surface layer is then going over to the roughness sublayer. The roughness sublayer can extend up to a height of 3 times the height of the canopy (Foken 2008, Kaimal and Finnigan 1994). The transport within the atmospheric surface layer is mainly dominated by turbulent processes. The exchange fluxes are only dominated by molecular processes a few mm closest to the surface of the ground (Foken 2008).

Table 2-1. The structure of the planetary boundary layer and the different processes affecting the exchange fluxes.

Height (m)	Layer	Exchange		Stability
<1,000	Ekman layer	Turbulent	No constant flux	Stability dependent
<100	Atmospheric surface layer (Inertial surface layer)	Turbulent	Flux constant	Stability dependent
~2.5 × plant canopy height	Atmospheric surface layer (Roughness sublayer)	Turbulent	No constant flux	Stability dependent
0.01	Viscous/laminar boundary layer	Molecular	Flux constant	Independent of stability

3 The inertial surface layer

3.1 Assumptions made for the eddy diffusivity approach to be valid

There are several processes affecting the motion of air in the atmosphere; tendency, advection, the pressure-gradient force, the Coriolis force, the molecular stress and the turbulent stress. Some of these terms are very small under certain circumstances and can then be neglected (Foken 2008). The tendency is negligible under steady-state flow. Above horizontally homogeneous surfaces, advection can be neglected. At the centre of high and low pressure areas and for small scale processes, pressure gradient forces can be neglected. It has also been shown that the pressure gradient force is only important in the upper part of the planetary boundary layer (Foken 2008). At the equator and for small scale processes, the Coriolis force can be neglected. The effect of the Coriolis force can also be neglected in the inertial surface layer, when it comes to the flux-gradient relationships (Foken 2008). It can however not be neglected in general, but as we are dealing with the vertical flux gradient relationship in this report, we can neglect it. In the inertial surface layer, the molecular viscosity is very small in comparison to the large scale movement due to turbulence, and can hereby be neglected. It is only important in the viscous/laminar boundary layer. However, the turbulent stress is relevant throughout the planetary boundary layer, and can hereby not be neglected. Under these circumstances it has been shown that the vertical gradients of the flux are zero, that is, the flux is constant (within 10%) (Foken 2008). This section of the atmosphere is called the inertial surface layer, or the constant flux layer. Another assumption done is that the mean vertical wind speed must be zero (Foken 2008). This is not the case in hilly terrain, and this is why the theories described in this report can only be applied above flat areas.

However, under steady state conditions, fully developed turbulent conditions, in flat and horizontal homogeneous areas in the inertial surface layer, it is possible to apply the eddy covariance and the K -theory for estimating vertical 2-dimensional fluxes. Steady state means that during the averaging period used for the estimates, there should not be any large change in the state variable that we are looking at. An easy way to test for steady state was proposed by Vickers and Mahrt (1997). For the wind, it can be tested by comparing the wind components at the beginning and the end of the time series:

$$\left| \frac{u_1 - u_n}{\bar{u}} \right| < 0.5 \quad (3-1)$$

where u_1 is the first measured wind speed (m s^{-1}) and u_n is the wind speed at the end of the measurement period. \bar{u} is the mean wind speed during the measurement period in the mean wind direction. To filter for fully developed turbulent conditions, it is often assumed that data measured with a friction velocity (u_* , see Section 3.2) lower than 0.1 should be rejected (Lund et al. 2007).

3.2 The wind profile under neutral conditions

There are frictional interactions between the surface of the ground and moving air in the atmosphere. This results in that closest to the surface (<0.01 m), the air is stationary. Then the further we move away from the ground, the more the wind speed increases. The frictional drag also results in that the air motion turns turbulent. Turbulence can be pictured as having many different irregular swirls, so called eddies, superimposed upon each other. Eddies can be a few mm to several kilometers in size.

Under neutral turbulent conditions, when potential air temperature is constant with height, the mean wind speed increases logarithmic with height:

$$\bar{u}(z) - \bar{u}(z_0) = \frac{u_*}{k} \times \ln\left(\frac{z}{z_0}\right) \quad (3-2a)$$

where u_* is the friction velocity (m s^{-1}), k is the von Karman constant, z is the height above ground (m), and z_0 is the roughness length (m) (Foken 2008). In this way air velocities in different layers in a stream can be compared when the stream is exposed to frictional forces. The von Karman constant is a dimensionless constant in the logarithmic velocity profile. Field measurements have reported values between 0.35 and 0.43, but 0.40 is the one that is mostly used today (Högström 1988). z_0 is the roughness length, that is the height where the wind velocity goes to 0 (Section 3.3, Figure 3-1). $\bar{u}(z_0)$ is hereby 0 and can thus be removed. Equation 3-2a hereby turns into:

$$\bar{u}(z) = \frac{u_*}{k} \times \ln\left(\frac{z}{z_0}\right) \quad (3-2b)$$

The friction velocity (u_*) is a very important parameter within micrometeorological theory. It is also called the shear velocity and it is derived from the shear stress. Shear stress exists when air is in turbulent motion. The turbulent eddies move parcels of air vertically, and air with different wind speed is hereby mixed. An air parcel moving into a section of the atmosphere with different wind speed will be deformed due to the velocity differences between different faces of the air parcel. This deformation is identical to if we would apply a force to the air parcel, i.e. a shear stress (Stull 1988). The air moving vertically (possessing vertical velocity w'), is mixed with air moving towards the air parcel (possessing u'). According to the eddy covariance theory, the momentum flux (F_m) can be estimated by taking the covariance of a state variable and the vertical wind velocity (Foken 2008):

$$F_m = \overline{u'w'} \quad (3-3)$$

where $u'w'$ is the covariance between the wind speed (m s^{-1}) in the horizontal (u) and the vertical (w) direction. The turbulent momentum flux hereby acts like a shear stress.

Shear stress arises from the force the ground friction exerts on the moving air in the atmosphere above the ground. It has been proven that the shear stress is an important scaling factor within micrometeorology. The shear stress is then changed to units of velocity:

$$u_* = \left(\frac{\tau}{\rho}\right)^{1/2} \quad (3-4)$$

where τ is the shear stress ($\text{kg m}^{-1} \text{s}^{-2}$) and ρ is the air density (kg m^{-3}). The friction velocity can also be calculated by taking the square root of the momentum flux:

$$u_*^2 = \overline{u'w'} \quad (3-5)$$

The friction velocity is a scaling parameter that has been shown to be very useful within micrometeorology.

3.3 The effect of plants and surface friction on the wind profile

The roughness of the ground surface needs to be considered. This is highly depending on the plant community and their height, density, shape and static stability. Equation 3-2 so far is only valid for soil areas without any plants. One thing that changes with a plant covered surface is the roughness length: the height where wind velocity becomes zero. It is not the same as the ground surface, but depending on the roughness of the surface, it is hereby different for different plant communities. It is a measure of how well the plant canopy dampens the wind speed. The roughness length has experimentally been set to approximately 1/10 of the height of the plants covering the surface (Foken 2008). Examples of roughness lengths in agricultural and forested areas are 0.16 m for wheat, 0.07 m for sugarbeets, 0.15 for grain, and 0.8–1.6 m for pine forests (Wieringa 1993). For lake or ocean surfaces it is usually set to 0.0001–0.001 (Foken 2008). The roughness length is the height where the logarithmic wind profile cuts the y-axis (Figure 3-1). Examples of the roughness length for several different plant communities is given by Wieringa (1993).

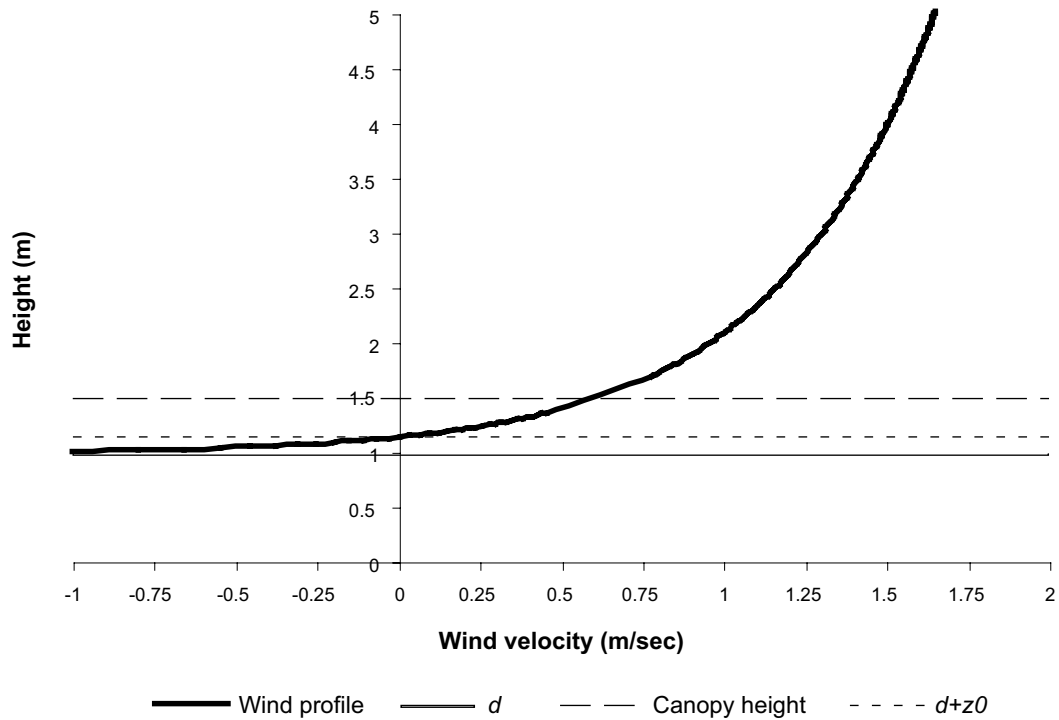


Figure 3-1. The wind profile under neutral conditions in the inertial surface layer above a plant community with 1.5 meters height. Friction velocity is set to 0.20. d is the zero plane displacement height and z_0 is the roughness length. Note that wind speed can not be negative; the negative section of the wind profile is only included to illustrate that the logarithmic curve levels out at the zero-plane displacement height.

However, the wind profile follows the logarithmic shape only above the canopy. In a dense canopy, the zero level of the wind velocity, that is, the height above the soil where the logarithmic profile levels out is no longer the ground. Therefore to account for the effect of the canopy height a parameter is included into equation 3-2b, the zero-plane displacement (d).

$$\bar{u}(z) = \frac{u_*}{k} \times \ln\left(\frac{z-d}{z_0}\right) \quad (3-6)$$

The zero-plane displacement (m) is the level to which the surface must be raised for the wind profile to follow a logarithmic shape (Figure 3-1). The zero plane displacement is slightly different for different plant canopies; it is set to 3/4 of the plant canopy height for forests (Kaimal and Finnigan 1994) whereas it can be 2/3 of the height for grassland and agricultural areas (Mölder et al. 1999).

3.4 The effect of diurnal variation on the wind profile

Until now, we have neglected the effect of air temperature, and buoyancy of the air. Warm air has lower density than cold air and therefore tends to rise through the atmospheric surface layer, whereas cold air is denser and therefore tends to sink in the atmospheric surface layer. The way the surface layer is heated up and cooled down over the 24-hour period is strongly dependent on the changes in solar radiation. The potential air temperature profile in the surface layer therefore has strong diurnal patterns, and this affects the wind profile.

Potential temperature is used instead of actual temperature as potential temperature is not affected by the change in temperature associated with pressure differences with different heights in the atmosphere. When an air parcel moves up a mountain it will expand and cool down, whereas when it descend on the other side of the mountain it compress and warms. However, the potential temperature will be the same for the parcel throughout this movement. Air parcels with the same potential temperature can be exchanged without any heating required. Whereas, air parcel with the

same actual temperature but at different heights, can not be exchanged without adding heat or work. In order not to introduce unstable conditions due to shifts in actual temperature with height, potential temperature is used:

$$\theta = T \times \left(\frac{P_0}{P} \right)^{R/c_p} \quad (3-7)$$

where θ is the potential temperature (K), T the actual temperature (K), P pressure (hPa), P_0 pressure at a reference height (hPa), R the universal gas constant ($\text{J kg}^{-1}\text{K}^{-1}$) and c_p is the specific heat capacity at constant pressure ($1,004.843 \text{ J kg}^{-1}\text{K}^{-1}$). Temperature increases with $\sim 1^\circ\text{C}$ per 100 meter and potential temperature can be approximated by:

$$\theta = T + 0.0098 \times z \quad (3-8)$$

where z is height above ground.

At night, the ground is usually colder than the air. An air package that is rising from the ground therefore soon encounters warmer air, and therefore stop rising. The turbulence is hereby dampened and the turbulence is therefore generally lower at night than during the day. These conditions are called stable conditions, i.e. the air temperature increases with height in the surface layer.

At sunrise, the sun starts to heat up the ground. The ground surface is heated up faster than the air. An air package above the ground surface is therefore warmer than the air above it. This warm air has higher buoyancy and it starts rise. When it rises, it comes across colder air and hereby continues to rise. The air flow in the surface layer becomes turbulent. The turbulence is increased and generally higher at daytime. These conditions are called unstable conditions, which mean that the potential air temperature decreases with height in the surface layer. The effect of the shear stresses due to friction of the ground is reduced with height, whereas the effect of buoyancy increases with height. The height of the atmospheric surface layer is therefore increased in daytime in comparison to nighttime.

During the evening, when the sun sets, the air temperature above the ground has the same temperature as the ground. The temperature profile then becomes adiabatic, and there is no exchange of heat. When the potential temperature is constant with height, conditions are neutral, and there is no turbulence caused by air parcels moving due to buoyancy differences.

3.5 Atmospheric stability parameter

In order to know if the conditions of the atmosphere are neutral, unstable or stable, we must know the effect of buoyancy on the turbulence of the atmosphere. There are many different parameters that describe the atmospheric stability. However, the one that is mostly used is called the Richardson's number. It is derived by comparing the contributions of buoyancy forces with the shear stress forces on the production of turbulent kinetic energy.

The production (or destruction) of turbulent kinetic energy due to shear stress is given by:

$$\frac{\partial \bar{e}_{friction}}{\partial t} = -\overline{u'w'} \times \frac{\partial \bar{u}}{\partial z} \quad (3-9)$$

where $\bar{e}_{friction}$ is the turbulent kinetic energy derived from shear stress, u' is the variance in wind velocity in the horizontal direction, w' is the variance in wind velocity in the vertical direction. This term can not destroy the turbulence as the shear stress is always a source of turbulence. It is always positive.

The production (or destruction) of turbulent kinetic energy due to buoyancy forces is given by:

$$\frac{\partial \bar{e}_{bouyancy}}{\partial t} = \frac{g}{T} \times \overline{w'\theta'} \quad (3-10)$$

where $\overline{e}_{\text{buoyancy}}$ is the turbulent kinetic energy derived from buoyancy forces, g is gravity (m s^{-2}), T is the air temperature and θ' is the variance in potential temperature. This term can be both positive and negative. In unstable conditions, gravitational (potential) energy is converted to kinetic energy, whereas under stable conditions it is the other way around; kinetic energy is converted into potential energy.

The flux Richardson's number is then calculated by taking the ratio of the buoyancy and the shear stress terms:

$$Ri_f = \frac{\frac{g}{T} \times \overline{w'\theta'}}{\overline{u'w'} \times \frac{\partial \overline{u}}{\partial z}} \quad (3-11)$$

We remove the negative sign in the denominator and it is hereby always negative. The sign of Ri_f is completely dependent on the sign of the nominator. When kinetic energy is produced by buoyancy forces, conditions are unstable, i.e. Ri_f will be negative (as the denominator is always negative). When the nominator is negative, kinetic energy is destroyed due to buoyancy forces. Ri_f is then positive and conditions are stable.

$Ri_f < 0$ for unstable conditions
 $Ri_f = 0$ for neutral conditions
 $0 < Ri_f < 1.0$, for stable conditions

Experimental observations have shown that turbulence cannot be maintained at $Ri_f > 1.0$. Above this value, buoyancy forces destroy so much turbulent kinetic energy that there are no longer turbulent conditions.

3.6 Monin-Obukhov similarity theory

The logarithmic wind profile (equation 3-6), is so far strictly only valid under neutral conditions. Monin and Obukhov used dimensional analysis according to Buckingham's Π theorem to make the equation also valid under unstable and stable conditions (Foken 2006). The dimensionless parameter derived is called the stability parameter (ζ):

$$\zeta = \frac{z - d}{L} \quad (3-12)$$

where z is the height above ground, d is the zero plane displacement height, and L is the Obukhov length (m). The Obukhov length can be estimated by:

$$L = - \frac{u_*^3}{\kappa \frac{g}{T} \frac{H}{\rho c_p}} \quad (3-13)$$

where c_p is the specific heat capacity of air at constant pressure ($\text{J kg}^{-1}\text{K}^{-1}$), and H is the sensible heat flux (W m^{-2}). Shear stresses are closest to the ground and buoyancy forces increases with height. The Obukhov length is proportional to the height above ground where production of turbulence by mechanical forces and loss of turbulence due to buoyancy forces are equal. This also means that L can be used to estimate stability:

$-10^5 < L < 0$ unstable conditions
 $0 < L < 10^5$ stable conditions
 $L < -10^5$ or $L > 10^5$ neutral conditions

3.7 Wind profiles under stable and unstable conditions

In unstable and stable conditions the wind velocity profile deviates from the simple logarithmic law. In these cases, Monin-Obukhov similarity theory is necessary for estimating the wind at different heights. This is done by using so called universal functions ($\varphi(\zeta)$). The differentiated form of the logarithmic wind profile, how the wind changes with height, then turns into:

$$\frac{\partial \bar{u}}{\partial z} = \frac{u_*}{k(z-d)} \times \varphi_m(\zeta) \quad (3-14)$$

The universal function has been determined in the field (Högström 1988) and the most common parameterisation today is:

$$\varphi_m(\zeta) = 1 + 6.0 \times \zeta \quad \text{for stable conditions } (\zeta > 0) \quad (3-15a)$$

$$\varphi_m(\zeta) = 1 \quad \text{for neutral conditions } (\zeta = 0) \quad (3-15b)$$

$$\varphi_m(\zeta) = (1 - 19.3 \times \zeta)^{-1/4} \quad \text{for unstable conditions } (\zeta < 0) \quad (3-15c)$$

When the atmospheric conditions are neutral, there is no stratification and the universal function is then 1. The logarithmic wind profile then turns into equation 3-6. However, to get the wind speed at a certain height, the logarithmic wind profile needs to be integrated. For the wind profile the integration from z_0 to z gives:

$$u(z) - u(z_0) = \frac{u_*}{k} \left[\ln \left(\frac{z-d}{z_0} \right) - \int \varphi_m(\zeta) d\zeta \right] \quad (3-16)$$

Equation 3-16 can be turned into:

$$u(z) = \frac{u_*}{k} \left[\ln \left(\frac{z-d}{z_0} \right) - \Psi_m(\zeta) \right] \quad (3-17)$$

where $\Psi_m(\zeta)$ is the integrated form of the universal functions.

$$\psi_m(\zeta) = -6.0 \times \zeta \quad \text{if } \zeta > 0, \text{ stable conditions} \quad (3-18a)$$

$$\psi_m(\zeta) = \ln \left[\left(\frac{1+x^2}{2} \right) \left(\frac{1+x}{2} \right)^2 \right] - 2 \tan^{-1} x + \frac{\pi}{2} \quad (3-18b)$$

where $x = (1 - 19.3 \times \zeta)^{1/4}$ if $\zeta < 0$, unstable conditions.

The Monin-Obukhov similarity theory has now given us a function where wind speed throughout the inertial surface layer can be calculated. Wind profiles in unstable, stable and neutral conditions are shown in Figure 3-2. We just need to know the friction velocity (u_*), the sensible heat flux (H), and the potential temperature (θ). The friction velocity and the sensible heat flux can be estimated from sonic anemometer three dimensional wind measurements. The potential temperature can be calculated from equations 3-7 or 3-8.

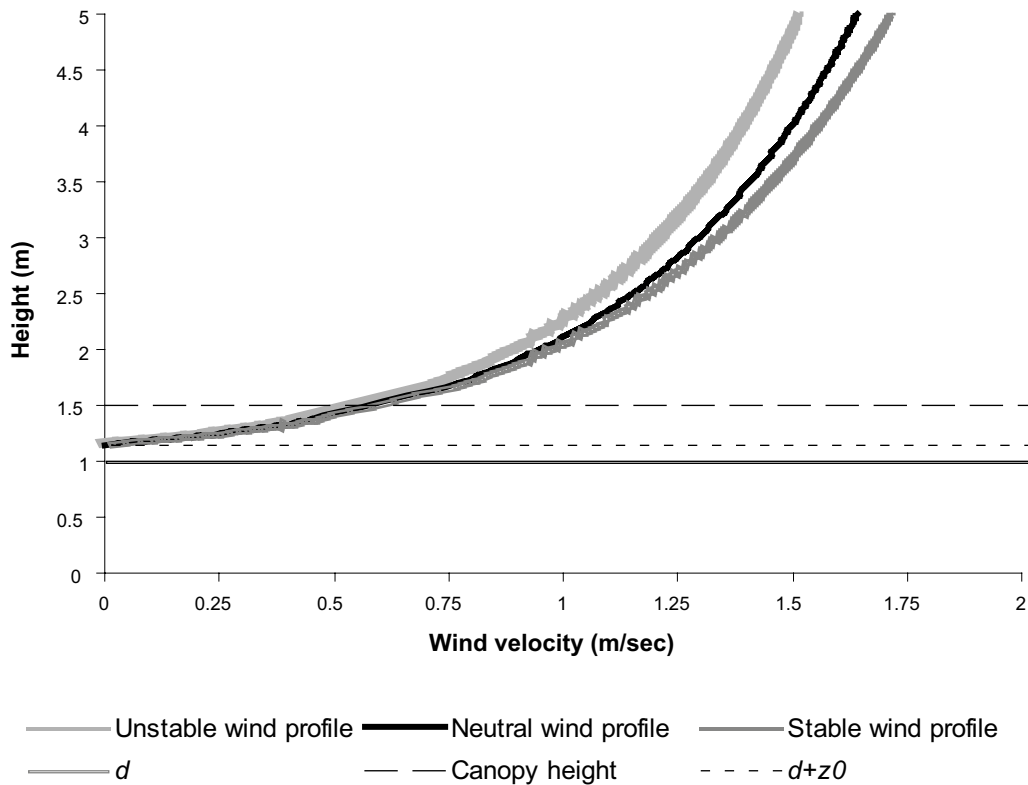


Figure 3-2. Unstable, neutral and stable inertial surface layer wind profiles above a plant community with 1.5 meters height. Friction velocity is set to 0.20. d is the zero plane displacement height and z_0 is the roughness length.

3.8 The eddy diffusion coefficient for momentum during neutral conditions

Molecules tend to move from an area with high concentration towards areas with lower concentration. This process is called molecular diffusion. Analogously to the molecular diffusion, it can be assumed that there is proportionality between vertical flux and the vertical gradient of a state variable (e.g. water vapour, CO₂ or heat) in the atmosphere. This proportionality constant is called the molecular diffusion coefficient in molecular processes, whereas it is called the eddy diffusion coefficient in the atmosphere. The motion within the atmosphere is not the same random motion of the molecules but rather irregular swirling turbulent motions of air parcels. The eddy diffusion coefficients are hereby much larger than the molecular diffusion coefficients. These irregular motions promote a mixing of the state variables in the inertial surface layer, in a similar way as the mixing due to molecular diffusion:

$$F = K \times \frac{\partial S}{\partial z} \tag{3-19}$$

where F is the flux (units $S \text{ m}^{-2} \text{ sec}^{-1}$), S is the state variable and z is the height above ground. The state variable can for example be momentum, temperature, water vapour and concentration of CO₂.

It is assumed that the flux is constant with height in the inertial surface layer. The concentration of the state variable is changing with height and this tells us that the eddy diffusion coefficients are also changing with height (equation 3-19).

So if we combine equation 3-3, 3-5, and the derivative of equation 3-6 (the change in wind speed with height) with equation 3-19, we get:

$$F_m = \overline{u'w'} = u_*^2 = K_m \frac{\partial \bar{u}}{\partial z} = K_m \frac{u_*}{k \times (z-d)} \quad (3-20)$$

This leads to that the eddy diffusion coefficient for momentum (K_m) can be estimated by:

$$K_m = k \times (z-d) \times u_* \quad (3-21)$$

3.9 The eddy diffusion coefficient for momentum during different stability conditions

To incorporate the effect of buoyancy on the eddy diffusivity coefficients (K), we need to apply Monin-Obukhov similarity theory to the model. This can be done by applying equation 3-14 with the universal functions to equation 3-20:

$$F_m = \overline{u'w'} = u_*^2 = K_m \frac{\partial \bar{u}}{\partial z} = K_m \frac{u_*}{k \times (z-d)} \times \varphi(\zeta) \quad (3-22)$$

This leads to that the eddy diffusion coefficient for momentum (K_m) can be estimated by:

$$K_{m(z)} = \frac{k \times (z-d) \times u_*}{\varphi_m(\zeta)} \quad (3-23)$$

Here we got a model for eddy diffusivity at a certain height. The momentum flux can now be estimated from:

$$F_m = K_m \frac{\partial \bar{u}}{\partial z} = \frac{k \times (z-d) \times u_*}{\varphi_m(\zeta)} \frac{\partial \bar{u}}{\partial z} \quad (3-24)$$

However, the eddy diffusivity is changing with height whereas the flux is constant in the inertial surface layer. To estimate eddy diffusivity of momentum in a layer in the atmosphere, equation 3-24 needs to be integrated between the top (z_2) and bottom (z_1) height of this layer:

$$F_m = (u_2 - u_1) \times \int_{z_1}^{z_2} \frac{k \times (z-d) \times u_*}{\varphi_m(\zeta)} dz \quad (3-25)$$

where u_1 and u_2 are wind speed at two different heights. By including the same integration as we did in Section 3.7, we get:

$$F_m = \frac{\kappa u_*}{\ln(z_2/z_1) - \psi_m(\zeta)_{z_2} + \psi_m(\zeta)_{z_1}} (u_2 - u_1) \quad (3-26)$$

where $\Psi_m(\zeta)$ is the integrated form of the universal functions (equation 3-18). By adding this new model for estimating momentum flux (F_m) to equation 3-24, we get:

$$F_m = K_m \frac{\partial \bar{u}}{\partial z} = K_m \frac{(u_2 - u_1)}{(z_2 - z_1)} = \frac{\kappa u_*}{\ln(z_2/z_1) - \psi_m(\zeta)_{z_2} + \psi_m(\zeta)_{z_1}} (u_2 - u_1) \quad (3-27)$$

This leads to that the eddy diffusion coefficient for momentum, K_m , in a layer between height z_2 and z_1 can be estimated by:

$$K_{m(z_2-z_1)} = \frac{\kappa \times u_* \times (z_2 - z_1)}{\ln(z_2/z_1) - \psi_m(\zeta)_{z_2} + \psi_m(\zeta)_{z_1}} \quad (3-28)$$

3.10 The temperature profile during different stability conditions

If all eddy diffusion coefficients would be the same, we would have our first model for calculating eddy diffusion coefficients. However, the eddy diffusion coefficient for momentum is not equal to the eddy diffusion coefficients for heat, water vapour and CO₂. The moving air parcels move more or less in a unit, and so does hereby the air properties within the air parcels (heat and gas concentrations). The eddy diffusion coefficient for estimating heat flux, called the sensible heat flux, can hereby also be used for the transport of CO₂. The actual movement (caused by the momentum) differs from these other properties of the air package.

From equation 3-5, it can be given that:

$$u_* = \frac{\overline{u'w'}}{u_*} \quad (3-29)$$

From this we can define similar scales, such as the potential temperature scale:

$$\theta_* = -\frac{\overline{\theta'w'}}{u_*} \quad (3-30)$$

This means that taking the scale of a state variable such as potential temperature, times the friction velocity will give flux of that state variable, in this case the sensible heat flux.

Similar with the wind profile (equation 3-6), the logarithmic temperature profile during neutral conditions is:

$$\overline{\theta}(z) - \overline{\theta}(z_{0T}) = \frac{\theta_*}{k} \times \ln\left(\frac{z-d}{z_{0T}}\right) \quad (3-31)$$

where z_{0T} is the temperature roughness length. Plant canopies are usually more efficient in absorbing momentum than absorbing heat. The temperature roughness length is therefore usually set to 1/5 of the roughness length for momentum (Kaimal and Finnigan 1994). However, values are different for different canopies depending on e.g. roughness and clumping of the plant canopy and radiation absorption efficiency. Foken (2008) sets the temperature roughness length to 1/10 of the roughness length of momentum. The temperature roughness length is the height to which the logarithmic temperature profile must be raised for the temperature to be the same as the true surface temperature.

In unstable and stable conditions the temperature profile deviates from the simple logarithmic law. In these cases, Monin-Obukhov similarity theory is necessary to apply for estimating the temperature at different heights. We therefore apply the universal functions on the differentiated form of the logarithmic temperature profile,

$$\frac{\partial \theta}{\partial z} = \frac{\theta_*}{k \times (z-d)} \times \varphi_H(\zeta) \quad (3-32)$$

This time it is the universal functions for the sensible heat exchanges that are incorporated. They have also been estimated in the field (Högström 1988) and the most common parameterization is:

$$\varphi_H(\zeta) = 0.95 + 7.8 \times \zeta \quad \text{for stable conditions } (\zeta > 0) \quad (3-33a)$$

$$\varphi_H(\zeta) = 1 \quad \text{for neutral conditions } (\zeta = 0) \quad (3-33b)$$

$$\varphi_H(\zeta) = 0.95 \times (1 - 11.6 \times \zeta)^{-1/2} \quad \text{for unstable conditions } (\zeta < 0) \quad (3-33c)$$

Again, when the atmospheric conditions are neutral, there is no stratification and the universal function is then 1. The logarithmic temperature profile then turns into equation 3-31. However, to get the temperature at a certain height, the logarithmic profile equation needs to be integrated. For the temperature profile the integration from z_{0T} to z gives:

$$\overline{\theta}(z) - \overline{\theta}(z_{0T}) = \frac{\theta_*}{k} \left[\ln\left(\frac{z-d}{z_{0T}}\right) - \int \varphi_H(\zeta) d\zeta \right] \quad (3-34)$$

Combining equation 3-30 with equation 3-34 gives:

$$\begin{aligned}\bar{\theta}(z) - \bar{\theta}(z_{0T}) &= \frac{\theta_*}{k} \left[\ln \left(\frac{z-d}{z_{0T}} \right) - \Psi_H(\zeta) \right] = \frac{\left(\frac{\overline{w'\theta'}}{u_*} \right)}{k} \left[\ln \left(\frac{z-d}{z_{0T}} \right) - \Psi_H(\zeta) \right] \\ &= \frac{\overline{w'\theta'} \times k}{u_*} \left[\ln \left(\frac{z-d}{z_{0T}} \right) - \Psi_H(\zeta) \right]\end{aligned}\quad (3-35)$$

where $\Psi_H(\zeta)$ is the integrated form of the universal functions:

$$\psi_H(\zeta) = -7.8 \times \zeta \quad \text{if } \zeta > 0, \text{ stable conditions} \quad (3-36a)$$

$$\psi_m(\zeta) = 2 \times \ln \left(\left(1 + 0.95 \times (1 - 11.6 \times \zeta)^{1/2} \right) / 2 \right) \quad \text{if } \zeta < 0, \text{ unstable conditions} \quad (3-36b)$$

3.11 The eddy diffusion coefficient for sensible heat during different stability conditions

The flux is defined as positive upwards, whereas negative when it is directed towards the ground. Temperature decreases with height (as do CO₂ and water vapour), and a negative sign is hereby introduced into our eddy diffusivity equation:

$$F_H = -K_H \frac{\partial \bar{\theta}}{\partial z} \quad (3-37)$$

where F_H is the sensible heat flux and K_H is the eddy diffusivity of sensible heat. Analogously to the momentum flux (equation 3-22), by combining equation 3-30, 3-37 and 3-32 we get:

$$F_H = \overline{\theta' w'} = -\theta_* \times u_* = -K_H \frac{\partial \bar{\theta}}{\partial z} = -K_H \frac{\theta_*}{k \times (z-d)} \times \varphi_H(\zeta) \quad (3-38)$$

This leads to that the eddy diffusion coefficient for sensible heat (K_m) can be estimated by:

$$K_H = \frac{k \times (z-d) \times u_*}{\varphi_H(\zeta)} \quad (3-39)$$

Here we got a model for eddy diffusivity at a certain height. The sensible heat flux can now be estimated from:

$$F_H = -K_H \frac{\partial \bar{\theta}}{\partial z} = -\frac{k \times (z-d) \times u_*}{\varphi_H(\zeta)} \frac{\partial \bar{\theta}}{\partial z} \quad (3-40)$$

As mentioned above, the eddy diffusivity is changing with height whereas the flux is constant in the inertial surface layer. To estimate eddy diffusivity in a layer in the atmosphere, equation 3-40 needs to be integrated between the top (z_2) and bottom (z_1) height of this layer.

$$F_H = -(\theta_2 - \theta_1) \times \int_{z_1}^{z_2} \frac{k \times (z-d) \times u_*}{\varphi_H(\zeta)} dz \quad (3-41)$$

where θ_1 and θ_2 are the potential temperatures at two different heights. By doing the same integration as we did in the Section 3.7, we get a model for estimating the sensible heat flux from measurements of temperature at two different levels.

$$F_H = -\frac{\kappa u_*}{\ln(z_2/z_1) - \Psi_H(\zeta)_{z_2} + \Psi_H(\zeta)_{z_1}} (\theta_2 - \theta_1) \quad (3-42)$$

where $\Psi_H(\zeta)_z$ is the integrated form of the universal functions at height z_1 and z_2 (equation 3-36). This new model for estimating sensible heat flux can be compared with equation 3-37:

$$F_H = -K_H \frac{\partial \bar{\theta}}{\partial z} = -K_H \frac{(\theta_2 - \theta_1)}{(z_2 - z_1)} = -\frac{\kappa u_*}{\ln(z_2/z_1) - \Psi_H(\zeta)_{z_2} + \Psi_H(\zeta)_{z_1}} (\theta_2 - \theta_1) \quad (3-43)$$

Then it is easy to extrapolate K_H , which gives an estimate of eddy diffusivity in a layer with height between z_2 and z_1 :

$$K_{H(z_2-z_1)} = \frac{\kappa \times u_* \times (z_2 - z_1)}{\ln(z_2/z_1) - \Psi_H(\zeta)_{z_2} + \Psi_H(\zeta)_{z_1}} \quad (3-44)$$

This has given us our first model to estimate eddy diffusion coefficients above the plant canopy in the inertial surface layer. $\Psi_m(\zeta)$ is the integrated form of the universal functions and it can be calculated with equation 3-36. The input data required for modeling eddy diffusivity with equation 3-44 is the sensible heat flux, friction velocity and the potential temperature. The sensible heat flux and the friction velocity can be estimated from 3 dimensional wind measurements from a sonic anemometer. Friction velocity can be estimated by taking the square root of equation 3-5 and sensible heat flux can be estimated by taking the covariance between potential temperature and vertical wind velocity (equation 3-38). Potential temperature can be calculated from air temperature measurements using equation 3-7 or 3-8.

3.12 Profile measurements for estimating eddy diffusivity

As described under Section 3.5, the flux Richardson's number can be calculated by taking the ratio of the buoyancy and the shear stress terms. In these terms, momentum and sensible heat flux is included. Instead of using flux data, it is possible to estimate Richardson's number from profile measurements of temperature and wind. In this way we can estimate stability without having sonic anemometer 3-d wind measurements. Instead of the flux Richardson's number, we get the gradient Richardson's number (Ri_g):

$$Ri_g = \frac{g}{T} \times \frac{\partial \bar{\theta}}{\partial z} \times \left(\frac{\partial \bar{u}}{\partial z} \right)^{-2} = \frac{g}{T} \times \frac{\Delta \bar{\theta}}{(\Delta u)^2} \times (z_2 - z_1) \quad (3-45)$$

where T is the average temperature of the two heights. As described under Section 3.6, the Obukhov length is proportional to the height above ground where production of turbulence by mechanical forces and loss of turbulence due to buoyancy forces are equal. By taking the height and divide it by the Obukhov length, we get the stability parameter (equation 3-12), which indicates the stability of the atmosphere at the height we are looking at. It has been shown that the stability parameter is identical to gradient Richardson's number under unstable conditions, whereas in stable conditions they can be converted (Foken 2008):

$$\zeta = Ri_g \quad \text{for} \quad Ri_g < 0 \quad (3-46a)$$

$$\zeta = \frac{Ri_g}{1 - 5Ri_g} \quad \text{for} \quad 0 < Ri_g < 0.2 \quad (3-46b)$$

From equation 3-46, it is possible to estimate the stability parameter from the gradient Richardson's number. When we have the stability parameter, we can estimate the universal functions, $\varphi_m(\zeta)$, using equation 3-15. Then u_* can be estimated by rearranging equation 3-14:

$$u_* = \frac{\partial \bar{u}}{\partial z} \times \frac{k(z-d)}{\varphi_m(\zeta)} \quad (3-47)$$

When we have both u_* and the stability parameter, the eddy diffusivity can be estimated from equation 3-44 in combination with equation 3-36. This is our second model to estimate eddy diffusivity in the inertial surface layer above the plant canopy. The required input data is average wind speed and potential temperature from at least two different heights above the canopy in the inertial surface layer. The different heights must be separated enough to get a proper estimate of the wind and temperature profile. The ratio between the two different heights should be at least 4, which makes this method mainly applicable over areas covered with low plant canopies.

The profile method requires that the temperature and the wind speed are measured at the same level. If this is not the case a different method could be used to estimate Obukhov length required for estimating atmospheric stability. This is based on an iteration technique. First friction velocity (u_*) (equation 3-47) and the temperature scale (θ_*) is calculated without any stability corrections ($\varphi_m(\zeta) = 1$). The temperature scale can be estimated by:

$$\theta_* = \frac{\partial \bar{\theta}}{\partial z} \times \frac{k(z-d)}{\varphi_H(\zeta)} \quad (3-48)$$

The u_* and θ_* estimates are then substituted into:

$$L = -\frac{\bar{T} u_*^2}{g k \theta_*} \quad (3-49)$$

and Obukhov length is calculated. This estimate of Obukhov length is then used in equation 3-47 in combination with equation 3-15, and in equation 3-48 in combination with equation 3-33. A new u_* and θ_* is hereby estimated. This is done a couple of times until the Obukhov length is converging. This method is fully explained in (Berkowicz and Prahm 1982). This article is rather old and some parameters (e.g. von Karmans constant and the universal functions) have been recalculated. The basic method in the article is still correct though.

4 The Roughness sublayer

“We will understand the movement of the stars long before we understand canopy turbulence”
(Galileo Galilei)

4.1 Characteristics of the roughness sublayer

In Section 3, we have studied flow above a horizontal homogeneous surface which extends without end in all directions. We have regarded all flow as 2 dimensional, as we are only looking at flow in the vertical direction. The logarithmic profiles with modifications due to atmospheric stability apply. Large eddies are formed because of the thermal kinetic energy created by shear stress and the buoyancy of air. This energy is then transported towards smaller eddies and differently sized eddies from mm to km in size are responsible for the turbulent transport. However, when we approach the top of the canopy, the situation gets complicated. The section of the atmosphere where the fluxes are affected by the canopy is called the roughness sublayer. The wind flow gets three dimensional, and wind and scalar gradients are influenced by effects of the plant canopy. The fluxes are no longer constant and we therefore leave the inertial surface layer (or the constant flux layer). The models described under Section 3 are therefore no longer valid. The roughness sublayer extends from the ground up to a height of ~ 3 times the height of the plant canopy (Foken 2008, Kaimal and Finnigan 1994).

When the mean wind interacts with the canopy, turbulence is created not only by shear stress and buoyancy as in the inertial surface layer. Turbulence is also created by wakes, which are formed behind the roughness elements, that is, tree stems, leafs and branches. This results in that turbulence is higher than it would be over a flat surface, and the turbulent transport is more efficient. The turbulence increases with density of roughness elements. The length of eddies formed by the wakes are approximately in the same scale as the length of the roughness elements (Kaimal and Finnigan 1994). There are perturbations on the mean wind gradient in the roughness sublayer, so that the gradient is lower than it is in the inertial sublayer; the mean wind profile is inflected (Figure 4-1).

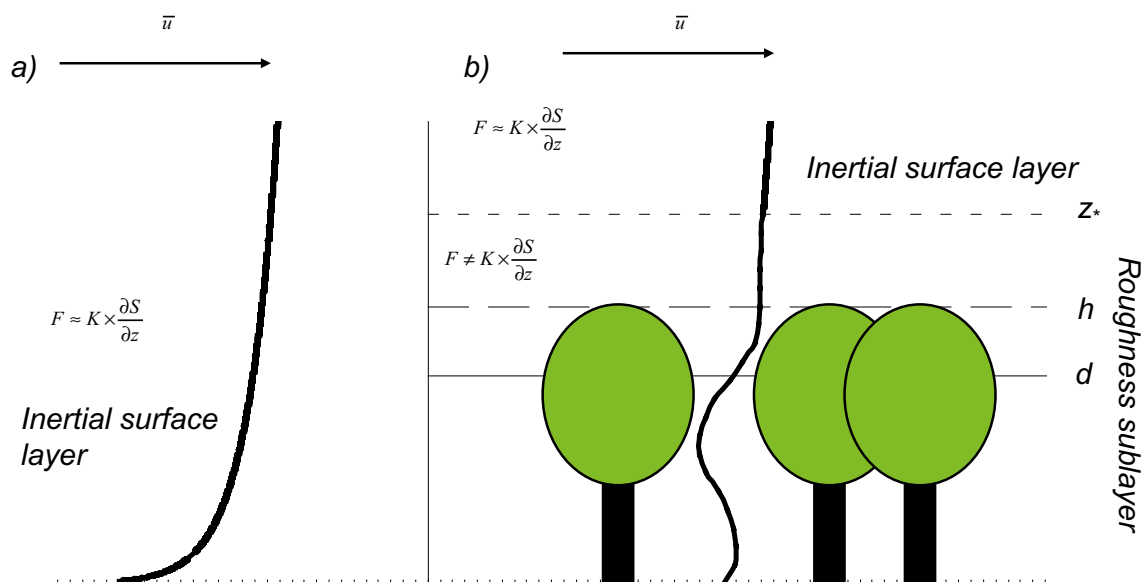


Figure 4-1. The mean wind profile above short vegetation (a) and above and within the roughness sublayer of a forest canopy (b).

Additionally, when the wind goes through the canopy, there is frictional drag, that is, friction between the bypassing air and the roughness elements. This results in that the kinetic energy in large sized eddies do not cascade into middle sized eddies, as in the inertial surface layer. This frictional drag results in that the energy cascade bypasses the middle sized eddies and small size eddies are directly formed. Therefore, large and small sized eddies are the main means of turbulent transport within the roughness sublayer. Energy is also dissipated as heat due to this frictional drag and due to fact that plants start to wave when the wind bypasses them (Kaimal and Finnigan 1994).

There is an interesting feature of the wind profiles within the roughness sublayer. Several different measurements from complex forests with large trees, from agricultural and grassland areas and from wind tunnel experiments using simple rods show very similar profiles of wind speed, within and immediately above the canopy when normalized by the canopy height (Kaimal and Finnigan 1994).

4.2 Turbulent transport above the canopy but within the roughness sublayer

According *K*-theory, the exchange processes of energy and matter are proportional to the gradient of the state parameter. Above the plant canopy, the profiles of the state parameters are modified because of the high turbulence caused by the high roughness in the vicinity of the plant canopy (Figure 4-1). The profile equations must therefore be changed, and this is done by including a function that compensate for the effect of the increased turbulence (Foken 2008).

$$F_H = - \frac{k \times (z - d) \times u_*}{\varphi_* \left(\frac{z}{z_*} \right) \times \varphi_H(\zeta)} \frac{\partial \bar{\theta}}{\partial z} \quad (3-50)$$

where $\varphi_* \left(\frac{z}{z_*} \right)$ is the correction function and z_* is the height of the roughness sublayer (m). The mean height of the roughness sublayer can be calculated as

$$z_* = h + D \quad (3-51)$$

where h is the height of the canopy (m) and D is the mean distance between the roughness elements (m) (Rannik et al. 2003). However, there is large temporal variation and as described above it can often be 3 times the height of the plant canopy (Foken 2008, Kaimal and Finnigan 1994).

$$\varphi_* \left(\frac{z}{z_*} \right) = \exp \left[-0.7 \times \left(1 - \frac{z}{z_*} \right) \right] \quad (3-52)$$

The eddy diffusion coefficients are hereby larger above the plant canopy within the roughness sublayer than in the inertial surface layer. This corrected version of the profile equation should always be used above high plant canopies; otherwise it will give incorrect results. However, this corrected version can only be used down to the height of the plant canopies, within the canopies other models needs to applied. Mölder et al. (1999) describe the roughness sublayer correction above the plant canopy accurately.

4.3 Turbulent transport within the plant canopy

The turbulent transport gets complicated when we enter the plant canopy, especially when it comes to transport of scalars, such as heat, water vapour and CO₂. The profiles are then not only affected by the changes in turbulence, but also by the spatial distribution of sinks and sources for heat and gases within the plant canopy. The exchange of carbon within the plant community mainly goes through the stomata of leafs. The sink and source distribution of CO₂ is hereby influenced by

vertical and horizontal distribution of leaf area density and radiation. Similar to the wind gradient, the concentration profiles are modified and transport coefficients are larger than in the inertial surface layer. This means that the flux-gradient relationship that was described in Section 3, based on the Monin-Obukhov similarity theory is no longer valid.

According to the *K*-theory, fluxes of energy and matter are proportional to the gradient of the parameter we are looking at. A central assumption is that there is a correspondence between the sign of the gradient and the direction of the flux. In the Uriarra forest, Denmead and Bradley (1987) showed that this assumption worked well above the forest canopy. However, at the bottom of the needled area and in the trunk space, observed fluxes went opposite, that is, against the gradient of the state parameter. This has been observed for both heat fluxes and CO₂ fluxes, and it is called counter gradient fluxes (Denmead and Bradley 1987, Foken 2008, Kaimal and Finnigan 1994, Raupach 1989a). When it comes to CO₂, the assumption of a gradient relationship within the canopy would mean that CO₂ respired from the ground would supply the photosynthetic need of the plant up to the level of CO₂ minimum. However, in the Uriarra forest, CO₂ fluxes measured below this point showed that there was a net downward flux of CO₂ also below this point (Denmead and Bradley 1987). Occasionally, as much as 40% of the CO₂ entering the canopy from above were transported to levels below the point of minimum CO₂ concentration (Denmead and Bradley 1987). The reason for the counter gradient fluxes is that there is a continuous displacement and dilution of CO₂ at all levels in the canopy caused by gusts (air descending into the canopy) and bursts (air escaping from the canopy). Gusts bring cool, dry air with low CO₂ concentration from above the canopy and bursts transport warm, moist air with high CO₂ concentration away from the canopy.

Above the canopy there is a continuous flux of air between the canopy and the free atmosphere. Within the canopy, fluxes are less frequent and has a higher intensity (Denmead and Bradley 1987). At 3 meters height in the Uriarra forest (15 m high canopy), it was shown that during a 15 minute measurement, all vertical air transport was associated with 5 flux events. Four of these were associated with gusts and only 1 with a burst (Denmead and Bradley 1987). The same thing has been shown in several other studies (Denmead and Bradley 1987), for example Shaw et al. (1983) showed that 50% of the momentum transfer took place in gusts that occupied only 6% of the time. It can further be shown that flux and the concentration profiles differ from each other. Most of the time there is a build up of heat and CO₂ within the plant canopy, and then there is a sudden burst that transports the scalar up in the atmosphere and away from the canopy. This results in that time averaged profiles of a scalar are more affected by the source and sink distribution of this scalar, than by the direction of the transport.

One more thing should be mentioned, the scale of the transporting eddies. It has been shown that the turbulence within the canopy is dominated by large eddies (Foken 2008, Kaimal and Finnigan 1994). These are formed in the shear layer in the upper part of the crown. When the wind and moving air outside the canopy hits the upper parts of the crown, eddies are formed that have about the same length scale as do the plant canopy. When these eddies pass a certain point in the plant canopy space, there is one of the gusts or bursts transporting the air. According the *K*-theory, the turbulent elements of the gradient transport must be small (smaller than the length scale which is required for measuring the gradient of the state parameter), as it should simulate random motions of a diffusion process. The application of *K*-theory and Monin-Obukhov similarity theory does hereby not give any meaningful results (Foken 2008, Kaimal and Finnigan 1994). Additionally, this mixing length that is required for the *K*-theory to be applicable do not make sense when there are sinks and sources within vertical distances that are much shorter than this mixing length (Denmead and Bradley 1987).

4.4 Carbon dioxide profiles within the plant canopy

The CO₂ profiles show distinct diurnal patterns. During daytime, the CO₂ profiles have a minimum within the plant canopy; the CO₂ concentration decreases from the ground and upwards, and it decreases from the atmosphere above the plant canopy and downwards into the canopy. The reason for this is the distribution of sources and sinks of CO₂ within the canopy. The ground of the soil is a source of CO₂ as carbon is decomposed by soil microorganisms and by respiration in the root cells of the vegetation.

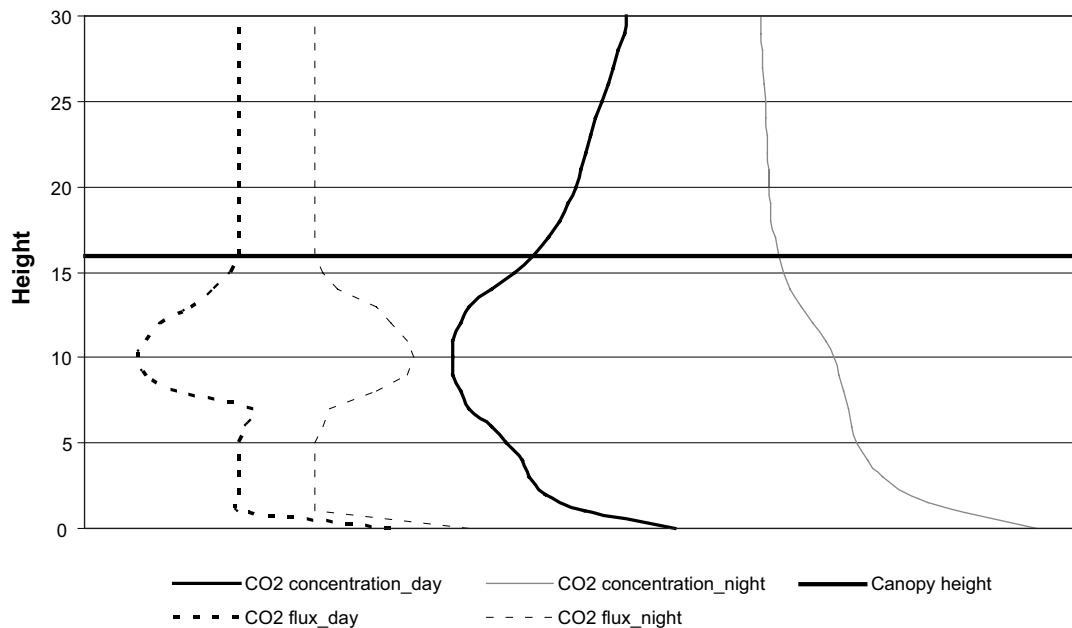


Figure 4-2. Examples of the mean CO_2 concentration and source and sink profiles of CO_2 within and above a plant canopy for day and night time.

Above the ground, there is, depending on plant community, a section with hardly any sinks or sources of CO_2 . This is the section of the canopy where there usually is a stem, which neither respire nor photosynthesize CO_2 . The allocation of sinks and sources within the canopy is then depending on the leaf area distribution. As we move upwards in the canopy there is an increase in the CO_2 uptake because of the increase in leaf area. The maximum uptake is at the height of the canopy where most leaves are situated, and most radiation is harvested. Then as we move upwards towards the top of the canopy, there is a decrease in leaf area. This result in a decrease in the CO_2 sink. These sources and sinks of CO_2 result in a concentration profile that is at a maximum above the canopy in the atmosphere and close to the soil surface (Figure 4-2) (Nobel 2009). During night, it is dark and there is hereby no photosynthesis within the plant canopy. There is therefore no sinks in CO_2 anywhere in the canopy, there are only sources, which results in that the CO_2 concentration is highest closer to the ground and it gets lower the further away from the CO_2 sources we get (Figure 4-2). There can be a small bump in the CO_2 profile at the height of the maximum leaf area due to increased sources of CO_2 . For agricultural areas, the CO_2 concentration profiles are described in Baldocchi et al. (1983). The CO_2 concentration profiles in both agricultural and forest areas are described in Denmead and Bradley (1987).

4.5 Alternative modelling approaches

We now have an eddy diffusivity model that works well for the atmosphere above the plant canopy, whereas it has been shown not to be applicable within the canopy. There are mainly two approaches for modeling turbulent transport within the plant canopy; the Eulerian and the Lagrangian. The Eulerian describe the transport of parcels of air past a fixed point in space. The Lagrangian method describes the transport of air with a coordinate system that moves with the air parcel. An aim here is to shortly describe the the Lagrangian method, for a full description of the mathematics and the equations behind it, see (Raupach 1989a, b).

The Lagrangian model aims to predict the probability that a moving air parcel in the canopy space will encounter a source or a sink of a specific scalar. If we are looking at CO_2 , the CO_2 concentration of this air parcel will decrease when it passes a leaf which is photosynthesizing (a sink) or increase if it passes a source, which respire CO_2 . The aim is to predict the resultant concentration of CO_2 of an air parcel at a specific distance downwind (Raupach 1989b). The method assumes that the transfer of a scalar released from a point source is statistically comparable to a dispersion of particles that pass

through that point in space, and thereafter carry this scalar. This means that the sinks and sources distributed throughout the canopy can be regarded as point sources producing plumes of particles travelling downwind from that point in space, carrying with them the scalar. These particles are then spread throughout the canopy by the turbulence. The concentration of the scalar at any point in the canopy is then the total average of these particles arriving from all sources to that point. It can also be seen as the average of all overlapping plumes at that point (Kaimal and Finnigan 1994).

The particle that is emitted from the point source is assumed to distribute according to a Gaussian distribution. The depth of the scalar plume can therefore be estimated from the standard deviation of the vertical velocity of the particles. This standard deviation is related to the standard deviation of the vertical wind speed. It can be shown that the distance from the plume can be divided into two different sections; the near field and the fare field. The near field is the part of the plume where the standard deviation of the vertical velocity of the particles is in the same order as the standard deviation of the vertical wind speed. In the near field, the plume grows almost linearly with time. The particles moves along straight lines away from the sink or source point in the canopy space. However, when the particles move into the fare field part of the plume, they start to depart from their straight lines movement and move more randomly. For travel times that are large, the relationship between the vertical flux and the concentration gradient can therefore be regarded as an eddy diffusivity process. This distance has been shown to be in the similar length as the height of the plant canopy. Any concentration profile within a plant canopy that has a sink or source point that is less than the height of the canopy away, is therefore within the near field of these sinks or sources. The concentration profiles is then the total averages of the more concentrated plumes from the near field sources and the more diffused plumes from the fare field sources. These more near-field plumes therefore dominate the appearance of the concentration profiles, whereas the fare field plumes dominate the total rate of spread, that is, the flux or the transport. These things are described more in detail in Kaimal and Finningan (1994) and Raupach (1989a, b).

Acknowledgements

I would especially like to thank Meelis Mölder, whom taught me everything I know about micro-meteorology. I would also like to thank Anders Löfgren, Rodolfo Avila, and Patrik Vestin who gave good comments on the manuscript.

References

SKB's (Svensk Kärnbränslehantering AB) publications can be found at www.skb.se/publications.

- Baldocchi D D, Verma S B, Rosenberg N J, 1983.** Microclimate in the soybean canopy. *Agricultural Meteorology* 28, 321–337.
- Berkowicz R, Prahm L P, 1982.** Evaluation of the profile method for estimation of surface fluxes of momentum and heat. *Atmospheric Environment* 16, 2809–2819.
- Denmead O T, Bradley E F, 1987.** On scalar transport in plant canopies. *Irrigation Science* 8, 131–149.
- Foken T, 2006.** 50 years of the Monin-Obukhov similarity theory. *Boundary-Layer Meteorology* 119, 431–447.
- Foken T, 2008.** *Micrometeorology*. Berlin: Springer.
- Högström U, 1988.** Non-dimensional wind and temperature profiles in the atmospheric surface layer: a re-evaluation. *Boundary-Layer Meteorology* 42, 55–78.
- Kaimal J C, Finnigan J J, 1994.** *Atmospheric boundary layer flows: their structure and measurement*. Oxford: Oxford University Press.
- Lund M, Lindroth A, Christensen T R, Ström L, 2007.** Annual CO₂ balance of a temperate bog. *Tellus B* 59, 804–811.
- Mölder M, Grelle A, Lindroth A, Halldin S, 1999.** Flux-profile relationships over a boreal forest-roughness sublayer corrections. *Agricultural and Forest Meteorology* 98-99, 645–658.
- Nobel P S, 2009.** *Physicochemical and environmental plant physiology*. 4th ed. San Diego: Academic Press.
- Rannik Ü, Markkanen T, Raittila J, Hari P, Vesala T, 2003.** Turbulence statistics inside and over forest: influence on footprint prediction. *Boundary-Layer Meteorology* 109, 163–189.
- Raupach M R, 1989a.** Applying Lagrangian fluid mechanics to infer scalar source distributions from concentration profiles in plant canopies. *Agricultural and Forest Meteorology* 47, 85–108.
- Raupach M R, 1989b.** A practical Lagrangian method for relating scalar concentrations to source distributions in vegetation canopies. *Quarterly Journal of the Royal Meteorological Society* 115, 609–632.
- Shaw R H, Tavangar J, Ward D P, 1983.** Structure of the Reynolds stress in a canopy layer. *Journal of Climate and Applied Meteorology* 22, 1922–1931.
- Stull R B, 1988.** *An introduction to boundary layer meteorology*. Dordrecht: Kluwer Academic Publishers.
- Vickers D, Mahrt L, 1997.** Quality control and flux sampling problems for tower and aircraft data. *Journal of Atmospheric and Oceanic Technology* 14, 152–526.
- Wieringa J, 1993.** Representative roughness parameters for homogeneous terrain. *Boundary-Layer Meteorology* 63, 323–363.

Appendix 1

Flux data for the region above the plant canopy is easy to find, and it is measured at several different locations around the world. Data can be either downloaded or asked for from the site investigators at the home page of IMECC (http://www.europe-fluxdata.eu/newtcdc2/IMECC-TCDC_home.aspx). It might also be some profile data available, but it is much more seldom measured. There are most likely no data available from common open source databases for agricultural areas. Data from Norrunda, a mixed coniferous forest in the vicinity of Forsmark, can be found at the database of NECC (dbnecc.nateko.lu.se). CO₂ profiles were also available from the Boreal Ecosystem-Atmosphere Study (BOREAS) from NASA. A full list of available data from BOREAS sites can be found at (http://daac.ornl.gov/cgi-bin/dataset_lister_new.pl?p=2#TF). I did not find any wind profiles at the site where CO₂ profiles were measured, but most likely there is turbulence measurements above the canopy and then the wind profiles can be modelled (Raupach 1989, b).